analytical chemistry

pubs.acs.org/ac Article

A Boric Acid-Functionalized Lanthanide Metal–Organic Framework as a Fluorescence "Turn-on" Probe for Selective Monitoring of Hg^{2+} and CH_3Hg^+

Hao Wang, Xiuli Wang, Maosheng Liang, Guang Chen, Rong-Mei Kong, Lian Xia,* and Fengli Qu*

Cite This: *Anal. Chem.* 2020, 92, 3366–3372 Read Online

ACCESS | Metrics & More | Article Recommendations | Supporting Information

ABSTRACT: Mercury detection remains an important task because of its high toxicity. Herein a new dual-signal probe based on a boric acid (BA)-functionalized lanthanide metal–organic framework (BA-Eu-MOF) was developed for the detection of Hg^{2+} and CH_3Hg^+ ions for the first time. The BA-Eu-MOF was synthesized by coordination of Eu^{3+} with 5-boronobezene-1, 3-dicarboxylic acid (5-bop) through a one-pot method. The 5-bop ligand not only acted as the "antenna" to sensitize the luminescence of Eu^{3+} but also provided reaction sites for Hg^{2+} and CH_3Hg^+. Owing to the electron-withdrawing effect of the BA group, the "antenna" effect of the ligand was passivating and the BA-Eu-MOF showed weak red emission in water. Upon addition of Hg^{2+} or CH_3Hg^+ into the system, a transmetalation reaction took place, i.e., BA groups were replaced by Hg^{2+} or CH_3Hg^+; therefore, the "antenna" effect of the ligand was triggered, leading to the enhancement of red emission. As Hg^{2+} or CH_3Hg^+ concentration increased, the red emission was gradually enhanced, and the color change was also observed with the naked eye under 365 nm ultraviolet light. Owing to the porous characteristics and the surface effect of the MOF, as well as the unique transmetalation reaction between the BA group and Hg^{2+} or CH_3Hg^+, the developed nanoprobe showed excellent characteristics for simultaneous detection of Hg^{2+} and CH_3Hg^+, such as simple preparation, convenient operation, "turn-on" signal output, high sensitivity, and selectivity. The unique features of the BA-Eu-MOF make it an attractive probe for monitoring Hg^{2+} and CH_3Hg^+.

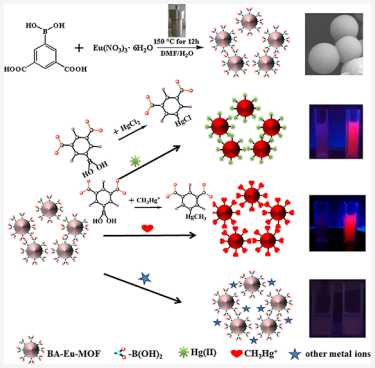

Mercury is a class of extremely toxic heavy metal pollutants and exists extensively in the ecosystem through numerous anthropogenic and natural sources.[1] The most common form of organic mercury, methylmercury (CH_3HgX; X = halide), is much more toxic than its inorganic form (HgX_2). Both Hg^{2+} and CH_3Hg^+ can accumulate in the human body through food chains and cause severe damage to nerves, digestion, kidney, cardiovascular, and endocrine systems even at trace levels.[2] Owing to the severely toxic characteristics and the trace lethal concentration of Hg^{2+} and CH_3Hg^+, highly sensitive, selective, and cost-effective methods for on-site detection are particularly needed.

However, detection of mercury, especially CH_3Hg^+ in real samples, remains a great challenge because of its trace level concentration and the variety of metal ion disturbances as well as lack of a special response site. Several facile and novel analytical methods for the detection of inorganic mercury Hg^{2+} have been established, including fluorescence,[3−5] electrochemical[6,7] and colorimetric[8−10] sensing probes, etc. Because mercury is a common quenching reagent, most sensors for mercury detection are signal "turn-off",[11,12] which suffer from more background disturbance than signal "turn-on" detection. Colorimetric methods based on gold nanoparticles show great potential due to unique characteristics, such as simple operation, on-site test, naked eye detection, etc. However, these methods are only used to detect inorganic Hg^{2+} ions. In fact, many reported sensing probes for mercury detection can only respond to inorganic Hg^{2+} ions, and few methods have been reported for CH_3Hg^+ detection. Therefore, development of convenient, selective, and sensitive methods with colorimetric signal output for detection of both organic and inorganic mercury at trace levels presents great challenges. An intelligent sensor playing a dual role of enrichment and special response site to target will be a perfect candidate.

Metal–organic frameworks (MOFs) have emerged as a class of promising and unique materials owing to their high porosity and large surface area.[13,14] MOFs have shown potential applications in the fields of gas storage,[15,16] separation,[17,18] sensors,[19−21] drug delivery,[22,23] catalysis, and biomimetics.[24−26] Especially, lanthanide MOFs (Ln-MOFs), formed by coordination of lanthanide metal ions to organic ligands, are generally preferred to construct skeletal materials having luminescent properties.[27−30] Luminescent Ln-MOFs exhibit unique fluorescent properties, such as large Stokes shifts, long

Received: November 29, 2019
Accepted: January 30, 2020
Published: January 30, 2020

https://dx.doi.org/10.1021/acs.analchem.9b05410
Anal. Chem. 2020, 92, 3366–3372

fluorescence lifetime, narrow emission spectra, etc. On the basis of these unique advantages, Ln-MOFs have drawn great attention for sensing applications.[31−34] It has been previously reported that MOFs functionalized by NH_2 or SH groups are high-efficiency probes for Hg^{2+} detection due to the interaction between Hg^{2+} ions and N, S.[35−37] However, these methods are based on the coordination of Hg^{2+} to amino or thiol groups, and other metal ions having similar electronic shell structures can influence detection.[38] Most importantly, although CH_3Hg^+ showed much more toxicity than Hg^{2+}, few probes have been reported for the detection of CH_3Hg^+, especially the simultaneous detection of Hg^{2+} and CH_3Hg^+. Therefore, development of MOF sensors with unique recognition sites for response to both CH_3Hg^+ and Hg^{2+} is greatly desired. Fortunately, phenylboronic acid showed a special activation of Hg^{2+} and CH_3Hg^+ through transmetalation. By C−B bond breaking and C−Hg bond forming, boric acid (BA) groups can be replaced by Hg^{2+} or CH_3Hg^+.[39−41] This is an important finding for mercury detection.

To take advantage of Ln-MOFs and the unique recognition of phenylboronic acid for Hg^{2+} and CH_3Hg^+, herein, on the basis of predecessors,[27] we compounded a BA-functionalized luminance MOF (BA-Eu-MOF) using Eu^{3+} as the metal node and 5-boronobezene-1,3-dicarboxylic acid (5-bop) as the ligand through a one-pot process for simultaneous monitoring of Hg^{2+} and CH_3Hg^+ in aqueous solution (Scheme 1). As shown in Scheme 1, the synthesized MOF showed sphere morphology with a uniform size and a diameter of about 400 nm. After incubation of the probe with Hg^{2+} or CH_3Hg^+, the transmetalation reaction occurred between the BA groups of the probe and the mercury ions; therefore, the red fluorescence emission of the probe was greatly enhanced. When other ions were incubated with the probe, the fluorescence emission exhibited no obvious change. The resultant probe not only offered a unique response site to Hg^{2+} and CH_3Hg^+ but also showed an enrichment effect to targets owing to the adsorption effect of MOF. Therefore, a "turn on" fluorometric and colorimetric probe based on BA-Eu-MOF has been developed for highly selective and sensitive detection of Hg^{2+} and CH_3Hg^+ ions in aqueous solution. Compared with previously reported UiO-66 @ Butyne,[3] N-CQD,[5] and other methods, the BA-Eu-MOF probe showed great advantages for mercury detection, such as simple preparation and operation, sensitive and selective response, fluorescent and colorimetric dual-signal output, simultaneous detection of organic and inorganic mercury, etc. The unique transmetalation reaction between the BA group and Hg^{2+} or CH_3Hg^+ can provide a potential strategy for the exploitation of promising sensing platforms for monitoring mercury ions.

Scheme 1. BA-Eu-MOF Synthesis and Representation of the Sensing Process of BA-Eu-MOF toward Hg^{2+} and CH_3Hg^+ Ions Based on Transmetalation

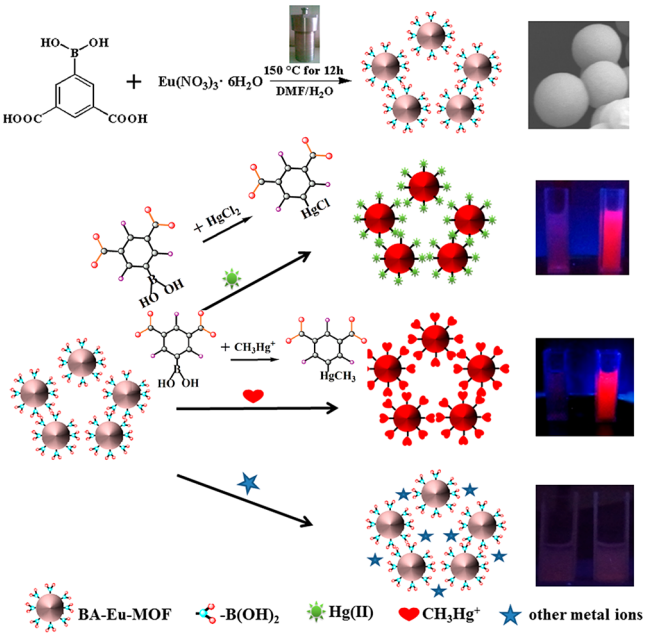

EXPERIMENTAL SECTION

Chemicals and Reagents. Europium(III) nitrate hexahydrate ($Eu(NO_3)_3·6H_2O$) was purchased from Aladdin (Shanghai, China). 5-Boronobezene-1,3-dicarboxylic acid (5-bop) was purchased from Zhengzhou Alpha Chemical Co., Ltd. (Zhengzhou, China). *N*,*N*-Dimethylformamide (DMF) and dichloromethane were purchased from Tianjin Chemical Reagent Co., Ltd. (Tianjin, China). Mercury chloride ($HgCl_2$) was purchased from Shandong West Asia Chemical Service Co., Ltd. (Linyi, China). Methylmercury (GSB 08675) and diphenylmercury (GSB 61851) were obtained from the National Institute of Metrology (Beijing, China). Phenylboronic acid (PBA) was purchased from Aladdin (Shanghai, China). The distilled water was purchased from Watson (Guangzhou, China). All chemical reagents were of analytical grade and used without further purification.

Instrumentation and Characterization. Thermal field emission scanning electron microscopy (SEM) (Carl Zeiss AG, Sigma 500 VP) and transmission electron microscopy (TEM) (JEOL, JEM-2100PLUS) were performed. Fourier transform infrared (FT-IR) spectra in the range of 4000−500 cm^{-1} were recorded on a Nicolet iS5 Fourier transform infrared spectrometer, and we used KBr pellets for tableting. A Bruker-500 MHz NMR (500 MHz/AVANCE III HD) was used. High performance liquid chromatography (HPLC) (Infinity II/1260) was performed. The UV detection was performed with a UV752pc spectrophotometer. Sample excitation wavelength, emission wavelength, and fluorescence detection were detected on a Hitachi F-7000 fluorescence spectrophotometer (emission slit width: 5 nm; excitation slit width: 10 nm; photomultiplier voltage: 400 V).

Preparation of BA-Eu-MOF. BA-Eu-MOF was prepared by a simple solvothermal method.[27] Briefly, 0.1 mmol of $Eu(NO_3)_3·6H_2O$ and 10 mmol of 5-bop were mixed in a beaker with 10 mL of DMF/H_2O (7:3, V/V), and then the mixture was stirred vigorously for 2 h on a magnetic stirrer. After that, the mixed solution was transferred into a Teflon vessel in a stainless steel autoclave and heated in an oven at 150 °C for 12 h. After the mixture was cooled to room temperature, the product was collected by centrifugation and washed with DMF and ethanol at least three times and then dried in an oven at 60 °C for 12 h. BA-Eu-MOF was collected as a white powder.

Fluorescence Sensing Experiment. Fluorescence response of BA-Eu-MOF toward aqueous solutions of various metal cations was investigated for their suspensions. The BA-Eu-MOF aqueous solution was first prepared by dispersing BA-Eu-MOF into water (0.3 mg/mL), and then the metal ions (Hg^{2+}, CH_3Hg^+, Ni^{2+}, Zn^{2+}, Ca^{2+}, Mg^{2+}, Al^{3+}, K^+, Mn^{2+}, Fe^{2+},

https://dx.doi.org/10.1021/acs.analchem.9b05410
Anal. Chem. 2020, 92, 3366−3372

Na^+, Ag^+, Zn^{2+}, Cd^{2+}, Co^{2+}, Pb^{2+}, and Cu^{2+}) were introduced into the aqueous solution to the final concentration of 120 μM at room temperature. The mixtures were modulated to pH 6 and then used for fluorescence measurements.

Determination of Hg^{2+} and CH_3Hg^+ in River Water Samples. The river water, obtained from the Dayi River (Qufu City, Shandong Province), was filtered through a cellulose membrane of 0.22 μm. Water samples containing different concentrations of Hg^{2+} or CH_3Hg^+ ions were prepared by spiking different amounts of Hg^{2+} or CH_3Hg^+ ions into the filtered river water and modulating the pH to 6 and then performing fluorescence detection.

RESULTS AND DISCUSSION

Sensing Mechanism. The as-synthesized BA-Eu-MOF showed characteristics of red light emission (fluorescence emission of Eu^{3+}), good dispersion, stability in water, etc. Owing to the electron-withdrawing effect of the BA group, the "antenna" effect of the ligand was passivating and the BA-Eu-MOF exhibited weak red emission in water. However, upon addition of Hg^{2+} or CH_3Hg^+ into the system, the spontaneous transmetalation reaction between Hg^{2+} or CH_3Hg^+ and BA groups took place, i.e., the C−B bond broke and the C−Hg bond formed.[39−41] Because the BA groups were replaced by Hg^{2+} or CH_3Hg^+, the electron-withdrawing effect from the BA group was lost and the "antenna" effect of the ligand was sensitized, leading to the enhancement of the red emission (Scheme 1). As Hg^{2+} or CH_3Hg^+ ion concentration increased, the red emission was gradually recovered, and the color change was observed with the naked eye under ultraviolet light at 365 nm. Owing to the porous characteristic and the surface effect of the MOF, as well as the unique transmetalation activity of BA groups with Hg^{2+} or CH_3Hg^+, this BA-Eu-MOF nanoprobe showed high sensitivity and selectivity to mercury.

Characterization of BA-Eu-MOF. The structural information on the prepared BA-Eu-MOF was investigated by SEM and TEM. As shown in Figure 1, the morphology of BA-Eu-MOF was a uniform nanosphere with an average diameter of about 400 nm. In addition, all the nanospheres were well-dispersed, which was beneficial for quick response to the targets.[27]

The FT-IR spectra were shown in Figure 2A. From Figure 2A, we can see that the peak of the ligand at 1695 cm^{-1}, which is derived from the C═O stretching vibration of the ligand, is missing in BA-Eu-MOF, indicating that the carboxyl groups were coordinated with Eu^{3+} to form BA-Eu-MOF. The absorption peak at 1313 cm^{-1}, which is derived from the BA group, was observed both in 5-bop and BA-Eu-MOF, suggesting that the BA-functionalized BA-Eu-MOF was successfully synthesized.[27] The absorption peak at 1583 cm^{-1} is the stretching vibration of C═C on the benzene ring. After Hg^{2+} was added, a new absorption peak at 1450 cm^{-1} was observed, which was derived from the stretching vibration of the C−Hg bond.[39] These results indicated that the transmetalation reaction between Hg^{2+} ions and BA-Eu-MOF took place.

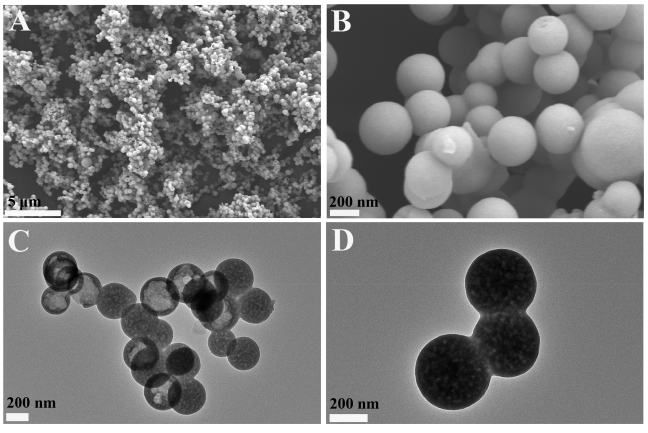

Figure 1. SEM images of BA-Eu-MOF with a ruler of 5 μm (A) and 200 nm (B). TEM images of BA-Eu-MOF with a ruler of 200 nm (C and D).

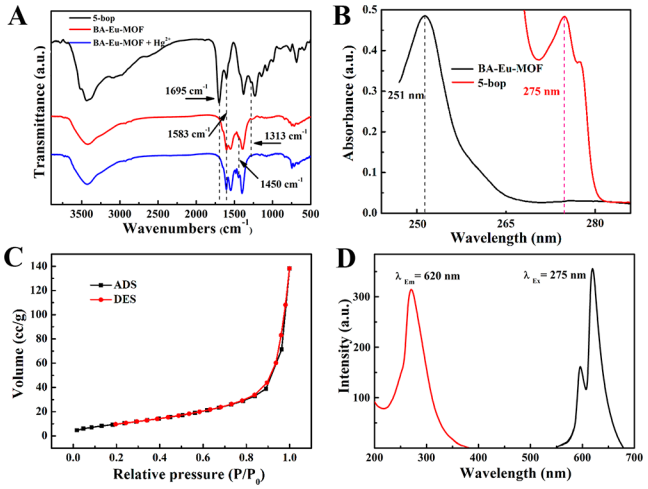

Figure 2. (A) FT-IR spectra of 5-bop (black), BA-Eu-MOF before (red) and after (blue) response to Hg^{2+}. (B) UV−vis spectra of 5-bop (red) (0.01 mg/mL) and BA-Eu-MOF (black) (0.05 mg/mL). (C) Nitrogen adsorption (ADS) and desorption (DES) curves. (D) Emission (Em) spectra of BA-Eu-MOF with λ_{Ex} = 275 nm (black); excitation (Ex) spectra of BA-Eu-MOF with λ_{Em} = 620 nm (red).

As shown in Figure 2B, BA-Eu-MOF exhibited absorption profiles similar to that of 5-bop, but there was about a 20 nm blue-shift after 5-bop was coordinated with Eu^{3+} to form BA-Eu-MOF. The porosity of the BA-Eu-MOF was confirmed by the N_2 sorption−desorption isotherm, and the result is shown in Figure 2C. According to the curve shape classified by IUPAC classification, this sorption−desorption process is classified as a type-V isotherm, indicating the weak interaction between BA-Eu-MOF and N_2. The BET surface area of the synthesized BA-Eu-MOF was measured by N_2 adsorption at 77 K. The results showed that the BET surface area was 39.7011 m^2/g. We also measured the excitation and emission wavelength of BA-Eu-MOF (Figure 2D). When excited with wavelength at 275 nm, the BA-Eu-MOF emitted red light at 620 nm.

Stability of BA-Eu-MOF. The stability of BA-Eu-MOF was investigated in aqueous solution, and the results are shown in Figure S1. As shown in Figure S1, the fluorescence intensity of BA-Eu-MOF suspension (0.3 mg/mL) at 620 nm showed negligible change after standing for 7 days, indicating the good day-to-day fluorescence stability in aqueous solution. Moreover, the characteristic emission of Eu^{3+} at 620 nm also exhibited satisfactory pH-independent stability in the pH range of 5−10 (Figure S2). The good fluorescence stability of the BA-Eu-MOF showed great potential for development of the probe in aqueous samples.

https://dx.doi.org/10.1021/acs.analchem.9b05410
Anal. Chem. 2020, 92, 3366−3372

Luminescence Properties of BA-Eu-MOF. The luminescent properties of BA-Eu-MOF were investigated at room temperature, and the results are shown in Figure 2D. From Figure 2D we can see that BA-Eu-MOF emitted two characteristic peaks at 595 and 620 nm, respectively, with excitation at 275 nm, which was derived from the $5D_0 \rightarrow 7F_1$ (595 nm) and $5D_0 \rightarrow 7F_2$ (620 nm) transitions of the Eu^{3+} ions. The main emission peak located at 620 nm corresponded to the transition of $5D_0$-$7F_2$ (electric dipole transition), suggesting that the "antenna" effect successfully occurred. Briefly, as shown in Scheme 2, the electron of the ligand (5-bop) was first excited to its S_1 state and was then followed by intersystem crossing to T_1 state. When nonradiative energy transferred from T_1 state of the ligand to Eu^{3+} ions, Eu^{3+} ion emission was observed.[27,29]

Scheme 2. Ligand−Metal Energy Transformation for Luminescence Emission and the Enhanced "Antenna" Effect of the Ligand Triggered by Hg^{2+} and CH_3Hg^+

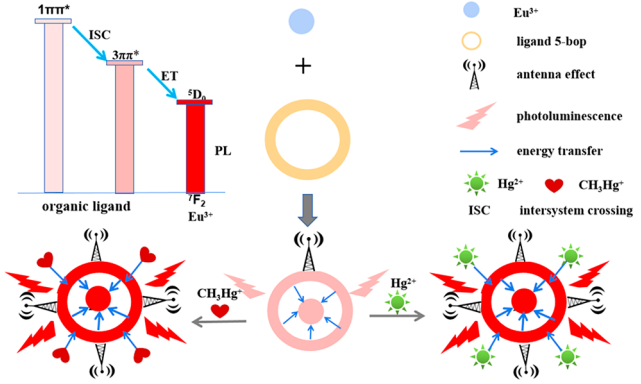

Sensing of Hg^{2+} and CH_3Hg^+ Ions. Taking advantage of the above characteristics, BA-Eu-MOF was utilized as a luminescence probe for the detection of Hg^{2+} and CH_3Hg^+. First, the response kinetics of the probe toward Hg^{2+} was investigated. With the concentration of Hg^{2+} at 60 μM, the fluorescence intensity of BA-Eu-MOF at 620 nm was measured with different response times. Figure 3 shows the fluorescence spectra of the detection system with different response times and the kinetics curve within 25 min. As shown in Figure 3, when the response time was less than 15 min, the fluorescence intensity of BA-Eu-MOF at 620 nm was enhanced gradually with an increase in response time and became constant when the response time reached 15 min. With continued increase in the response time, the fluorescence intensity showed no obvious increase. Similarly, the response kinetics of the probe toward CH_3Hg^+ ions was also investigated. CH_3Hg^+ ions were first dissolved in methanol and then were diluted greatly with water to different concentrations. The influence of methanol on the fluorescence of BA-Eu-MOF was then investigated. The results showed that methanol had no influence on the fluorescence of BA-Eu-MOF (Figure S3). As shown in Figure 4, the fluorescence intensity of BA-Eu-MOF at 620 nm became constant when the response time reached 20 min. These results indicated that Hg^{2+} and CH_3Hg^+ ions can respond quickly to BA-Eu-MOF, indicating feasibility of the sensor for detecting Hg^{2+} and CH_3Hg^+.

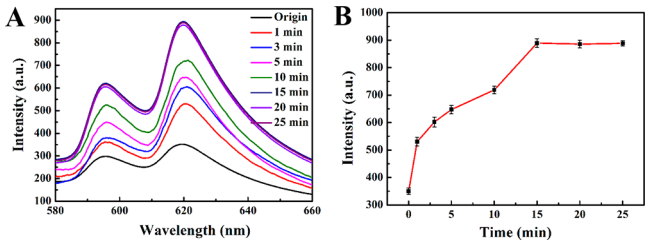

Figure 3. (A) The fluorescence intensity of BA-Eu-MOF (0.3 mg/mL) at 620 nm response with 60 μM Hg^{2+} ions with different response times. (B) Linear relationship between the fluorescence intensity at 620 nm and response time.

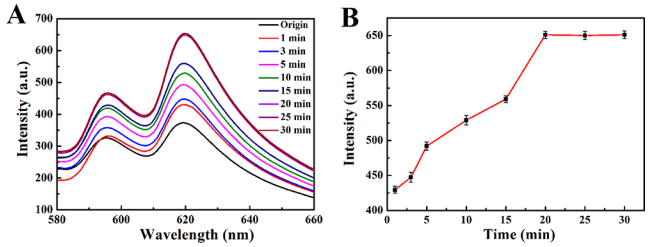

Figure 4. (A) The fluorescence intensity of BA-Eu-MOF (0.3 mg/mL) at 620 nm response with 60 μM CH_3Hg^+ ions with different response times. (B) Linear relationship between the fluorescence intensity at 620 nm and response time.

The pH value is an important factor for sensors; therefore, the influence of pH value on the fluorescent emission of the detection system was investigated. The fluorescence of BA-Eu-MOF in response to Hg^{2+} (120 μM) in aqueous solution under different pH values was studied, and the results are shown in Figure S4. From Figure S4A, we can see that the highest fluorescence intensity was achieved at pH values of 6 and 7. To achieve sensitive signal response for the detection of Hg^{2+}, the fluorescence intensity before and after adding Hg^{2+} at a pH value of 6 or 7 was compared, and the results are shown in Figure S4B. It can be seen from Figure S4B, the highest sensitive signal response was achieved at a pH value of 6. Therefore, the pH value of 6 was chosen as the optimal pH in the following detection work.

After the optimal conditions were obtained, the detection of Hg^{2+} and CH_3Hg^+ was then carried out. In the presence of different concentrations of Hg^{2+} or CH_3Hg^+ ions, the fluorescence intensity at 620 nm of BA-Eu-MOF (0.3 mg/mL) was measured after 15 min (CH_3Hg^+, 20 min) at pH 6. From Figure 5A/6A, it can be seen that the fluorescence intensity at 620 nm enhanced gradually with the increase in concentration in the range of 0−240 μM for Hg^{2+} and 0−200 μM for CH_3Hg^+. As shown in Figure 5B, the fluorescence intensity showed a good linear relationship versus the concentration of Hg^{2+} in the range of 1−60 μM with a linear correlation coefficient (R^2) of 0.9905, indicating a good linear relationship between Hg^{2+} ion concentration and fluorescence intensity. Similarly, the fluorescence intensity showed a good linear relationship versus the concentration of CH_3Hg^+ in the range of 2−80 μM (Figure 6B), and the linear correlation coefficient (R^2) was 0.9998, indicating a good linear relationship between CH_3Hg^+ ion concentration and fluorescence intensity. Figure 5C and Figure 6C show photographs of the detection system at various concentrations of Hg^{2+} and CH_3Hg^+ under UV light at 365 nm, respectively. Based on the signal-to-noise ratio of S/k = 3, the limit of detections

https://dx.doi.org/10.1021/acs.analchem.9b05410
Anal. Chem. 2020, 92, 3366−3372

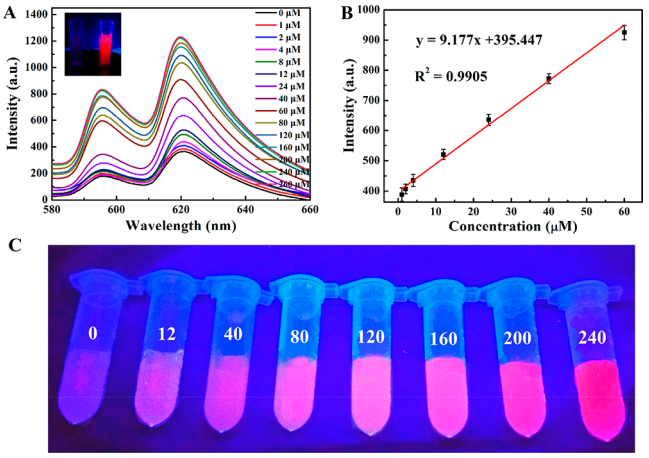

Figure 5. (A) The fluorescence spectra of BA-Eu-MOF under different concentrations of Hg^{2+} in aqueous solution; inset: before (left) and after (right) adding Hg^{2+} ions. (B) Linear relationship between the fluorescence intensity at 620 nm and Hg^{2+} ion concentration. (C) Photographs of the detection system of BA-Eu-MOF (0.3 mg/mL) in response to different concentrations of Hg^{2+} (0−240 μM) for 15 min under UV light at 365 nm.

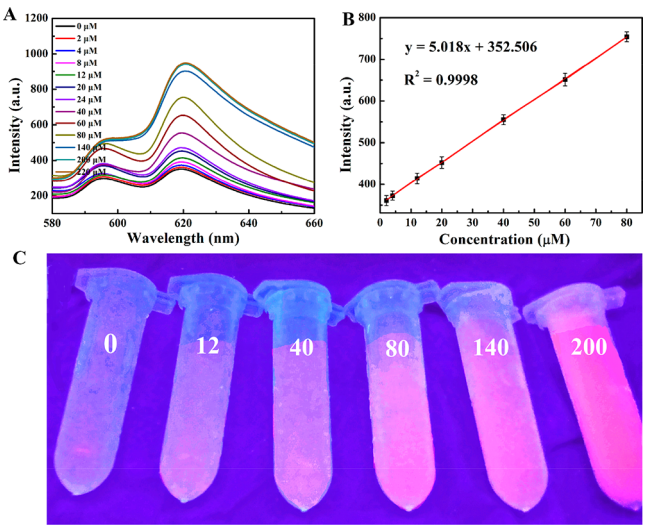

Figure 6. (A) The fluorescence spectra of BA-Eu-MOF under different concentrations of CH_3Hg^+ in aqueous solution. (B) Linear relationship between the fluorescence intensity at 620 nm and CH_3Hg^+ ion concentration. (C) Photographs of the detection system of BA-Eu-MOF (0.3 mg/mL) in response to different concentrations of CH_3Hg^+ (0−200 μM) for 20 min under UV light at 365 nm.

(LODs) of Hg^{2+} and CH_3Hg^+ were calculated to be 220 nM and 440 nM, respectively. By comparison with other reported methods, this established sensor showed several advantages, such as simultaneous detection of both Hg^{2+} and CH_3Hg^+, turn-on signal output, high sensitivity, wide detection range, facility, naked eye detection, etc. (Table S1).

Selectivity Study. To verify the specific recognition of BA-Eu-MOF toward Hg^{2+} and CH_3Hg^+ ions, a series of fluorescence tests in the presence of various metal ions were performed, and the results are shown in Figure 7. The results showed that under the same conditions, only Hg^{2+} and CH_3Hg^+ lead to remarkable fluorescence enhancement, while other metal ions (Ni^{2+}, Zn^{2+}, Ca^{2+}, Mg^{2+}, Al^{3+}, K^+, Mn^{2+}, Fe^{2+}, Na^+, Ag^+, Zn^{2+}, Cd^{2+}, Co^{2+}, Pb^{2+}, and Cu^{2+}) showed negligible

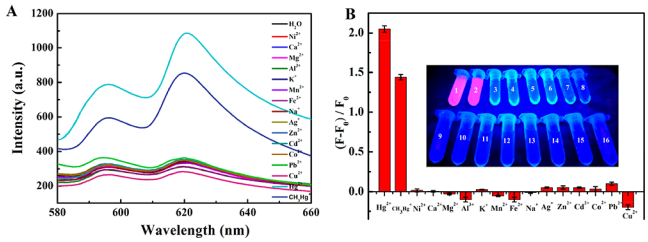

Figure 7. (A) Fluorescence spectra of BA-Eu-MOF toward various metal ions at the same concentrations (120 μM). (B) $(F - F_0)/F_0$ of different metal ions; the inset shows the detection system of BA-Eu-MOF (0.3 mg/mL) in response to 120 μM concentrations of different metal ions under UV light at 365 nm (the white numbers correspond to the ions below from left to right).

influence on fluorescence intensity of the BA-Eu-MOF. Especially, Cu^{2+}, Al^{3+}, and Fe^{2+} ions led to slight fluorescence quenching. The selectivity of the BA-Eu-MOF to Hg^{2+} and CH_3Hg^+ in the presence of interference ions was also examined, and the results are shown in Figure S5. As we can see in Figure S5, the probe still exhibited high selectivity for Hg^{2+} or CH_3Hg^+ ions in the presence of other interference ions. In addition, the selectivity of the probe was also examined with other species that may be present in natural water samples, such as humic acid and fulvic acid. As shown in Figure S6, these substances showed negligible effect on the fluorescence intensity of BA-Eu-MOF. Furthermore, as shown in Figure S7, the response of the BA-Eu-MOF probe to different sources of Hg^{2+} has been investigated using $HgCl_2$ with inorganic anions of MnO_4^- (oxidative anion) and NO_2^{2-} (reductive anion) as representatives. The results showed that both the oxidative anion of MnO_4^- and the reductive anion of NO_2^{2-} have almost no influence on the fluorescence intensity of BA-Eu-MOF. This revealed that BA-Eu-MOF exhibited high specific recognition of Hg^{2+} and CH_3Hg^+.

Transmetalation Reaction Mechanism Investigation. To investigate the transmetalation reaction of Hg^{2+} or CH_3Hg^+ ions with the probe, we employed PBA as the substrate to react with the Hg^{2+} or CH_3Hg^+ ions. Because the carboxyl groups of the ligand 5-bop coordinated with Eu^{3+} to form BA-Eu-MOF, we just investigated the reaction activity of the BA groups on the benzene ring. We used PBA to take the place of 5-bop in the mechanism study. After adding 1 mL of mercury chloride (5 mM) to 4 mL of PBA (1 mg/mL) aqueous solution at pH 6, the mixture was allowed to stand for 15 min, and then the floccule was collected by centrifugation and washed with deionized water three times and dried at 40 °C. The resulting product was subjected to ^1H NMR spectroscopy. As shown in Figure S8, the ^1H NMR characteristics of PBA are as follows: ^1H NMR (DMSO-d_6, 500 MHz): δ 7.44 (d, J = 6.5 Hz, 2H), 7.31−7.27 (m, 3H), 3.32 (s, 2H); the ^1H NMR characteristics of the reaction product (diphenylmercury) are as follows: ^1H NMR (DMSO-d_6, 500 MHz): δ 7.89−7.88 (m, 1H), 7.79−7.77 (m, 1H), 7.39−7.31 (m, 3H). Comparing the ^1H NMR spectra of PBA and the product, we found that the hydrogen on BA disappeared, which indicated that the BA groups were cleaved from the benzene ring after adding mercury ions.

To further verify that the BA groups were replaced by mercury ions, HPLC was performed with PBA standard and diphenylmercury. As shown in Figure S9A,B, the retention times of diphenylmercury and PBA were 10.7 and 4.1 min, respectively. From Figure S9C, we can see that the

https://dx.doi.org/10.1021/acs.analchem.9b05410
Anal. Chem. 2020, 92, 3366−3372

diphenylmercury peak at 10.7 min was observed after PBA reacted with Hg^{2+}, which indicated that the BA group was cleaved from the benzene ring and that the mercury ions connected to the benzene ring successfully. From Figure S9D, we can see that a new chromatographic peak at 2.6 min appears after PBA reaction with CH_3Hg^+, which was concluded to be methylphenylmecury. In addition, the IR spectra of diphenylmercury and the reaction product of PBA with Hg^{2+} also indicated that the C−Hg bond (1450 cm^{-1}) formed (Figure S10). Therefore, all these results showed that mercury ions can easily replace the BA groups on the benzene ring under the optimized conditions.

Practical Application. To verify the reliability and accuracy of BA-Eu-MOF for quantitative detection of Hg^{2+} and CH_3Hg^+ ions in real water samples, the BA-Eu-MOF probe was used to detect Hg^{2+} and CH_3Hg^+ ions in river water samples. To record the original content of the targets, the sensing performance was carried out with original water samples. The results showed that there were no mercury ions in the river water tested. Then the original water samples were spiked with different concentrations of the standard, and the sensing process was performed. The experimental results are shown in Table 1. As shown in Table 1, satisfactory recoveries (90.6−102.3%) and good analytical precision were achieved, which further confirmed the reliability of the BA-Eu-MOF probe for monitoring Hg^{2+} and CH_3Hg^+ ions in water samples.

Table 1. Detection of Hg^{2+} (samples 2, 3, 4) Ions and CH_3Hg^+ (samples 5, 6, 7) in Real Water Samples

sample	added (μM)	found (μM)	recovery (%)	RSD (%,n = 3)
1	0	0	–	–
2	5	4.53	90.6	3.16
3	10	10.23	102.3	2.35
4	15	15.26	101.7	2.04
5	5	4.63	92.6	3.14
6	10	9.76	97.6	2.78
7	15	15.34	102.2	1.85

CONCLUSIONS

To summarize, we have developed a BA-functionalized lanthanide metal−organic framework (BA-Eu-MOF) as a fluorescent nanoprobe for selective and sensitive detection of Hg^{2+} and CH_3Hg^+ in aqueous solution. The synthesized BA-Eu-MOF displayed uniform nanosphere morphology, high stability, porous property, and red fluorescence emission. The fluorescence intensity of as-prepared BA-Eu-MOF was sensitive toward Hg^{2+} in the linear range from 1 to 60 μM with an LOD of 220 nM and was also sensitive toward CH_3Hg^+ in the linear range from 2 to 80 μM with an LOD of 440 nM. Moreover, the specificity is an upshot of the fact that Hg^{2+} and CH_3Hg^+ are only capable of fast transmetalation with the boronic acid group of BA-Eu-MOF under various potential interfering ions. When the proposed probe was applied to detect Hg^{2+} and CH_3Hg^+ in real water samples, satisfactory results were achieved. By comparison with other fluorescence probes for detection of mercury, our probe exhibited advantages of a "turn on" signal, excellent anti-interference ability, and the capability for detecting Hg^{2+} and CH_3Hg^+ simultaneously in aqueous samples with a wide detection range. These results indicated that this BA-Eu-MOF nanoprobe possesses potential applications for Hg^{2+} and CH_3Hg^+ monitoring in a wide variety of environmental and biological samples.

ASSOCIATED CONTENT

Supporting Information

The Supporting Information is available free of charge at https://pubs.acs.org/doi/10.1021/acs.analchem.9b05410.

Day-to-day fluorescence stability of 0.3 mg/mL BA-Eu-MOF in water. Fluorescence spectra of BA-Eu-MOF (0.3 mg/mL) in aqueous solution with different pH values. The fluorescence intensity of BA-Eu-MOF at 620 nm response to methanol. NMR spectra of raw material (A) and possible product (B). Comparison of Hg^{2+} sensors based on various materials (PDF)

AUTHOR INFORMATION

Corresponding Authors

Lian Xia − *Key Laboratory of Life-Organic Analysis of Shandong Province, Qufu Normal University, Qufu, P.R. China;* orcid.org/0000-0001-6117-7596; Email: xialian01@163.com

Fengli Qu − *Key Laboratory of Life-Organic Analysis of Shandong Province, Qufu Normal University, Qufu, P.R. China;* orcid.org/0000-0001-6311-3051; Phone: +86 537 4456301; Email: fengliquhn@hotmail.com; Fax: +86 537 4456301

Authors

Hao Wang − *Key Laboratory of Life-Organic Analysis of Shandong Province, Qufu Normal University, Qufu, P.R. China*

Xiuli Wang − *Key Laboratory of Life-Organic Analysis of Shandong Province, Qufu Normal University, Qufu, P.R. China*

Maosheng Liang − *Key Laboratory of Life-Organic Analysis of Shandong Province, Qufu Normal University, Qufu, P.R. China*

Guang Chen − *Key Laboratory of Life-Organic Analysis of Shandong Province, Qufu Normal University, Qufu, P.R. China;* orcid.org/0000-0002-0454-1686

Rong-Mei Kong − *Key Laboratory of Life-Organic Analysis of Shandong Province, Qufu Normal University, Qufu, P.R. China*

Complete contact information is available at: https://pubs.acs.org/10.1021/acs.analchem.9b05410

Author Contributions

All authors have given approval to the final version of the manuscript.

Notes

The authors declare no competing financial interest.

ACKNOWLEDGMENTS

This work is supported by grants awarded by the National Natural Science Foundation of China (nos. 21505084, 21775089), Natural Science Foundation Projects of Shandong Province (ZR2014BM029), Key Research and Development Program of Shandong Province (no. 2017GSF19109), Innovation Project of Shandong Graduate Education (no. SDYY16091), Outstanding Youth Foundation of Shandong Province (ZR2017JL010) and Taishan Scholar of Shandong Province.

REFERENCES

(1) Liu, B. H.; Liu, D. X.; Yang, K. Q.; Dong, S. J.; Li, W.; Wang, Y. J. *Inorg. Chem. Commun.* **2018**, *90*, 61−64.

(2) Clarkson, T. W.; Magos, L.; Myers, G. J. *N. Engl. J. Med.* **2003**, *349*, 1731−1737.
(3) Samanta, P.; Desai, A. V.; Sharma, S.; Chandra, P.; Ghosh, S. K. *Inorg. Chem.* **2018**, *57*, 2360−2364.
(4) Razavi, S. A. A.; Masoomi, M. Y.; Morsali, A. *Inorg. Chem.* **2017**, *56*, 9646−9652.
(5) Zhang, R.; Chen, W. *Biosens. Bioelectron.* **2014**, *55*, 83−90.
(6) Liu, Z.; Puumala, E.; Chen, A. *Sens. Actuators, B* **2019**, *287*, 517−525.
(7) Tamiji, T.; Nezamzadeh-Ejhieh, A. *Electrocatalysis* **2019**, *10*, 466−476.
(8) Du, J.; Wang, Z.; Fan, J.; Peng, X. *Sens. Actuators, B* **2015**, *212*, 481−486.
(9) Lai, C.; Qin, L.; Zeng, G.; Liu, Y.; Huang, D.; Zhang, C.; Xu, P.; Cheng, M.; Qin, X.; Wang, M. *RSC Adv.* **2016**, *6*, 3259−3266.
(10) Xu, X. Y.; Yan, B. *J. Mater. Chem. C* **2016**, *4*, 1543−1549.
(11) Das, A.; Banesh, S.; Trivedi, V.; Biswas, S. *Dalton Trans.* **2018**, *47*, 2690−2700.
(12) Rudd, N. D.; Wang, H.; Fuentes-Fernandez, E. M. A.; Teat, S. J.; Chen, F.; Hall, G.; Chabal, Y. J.; Li, J. *ACS Appl. Mater. Interfaces* **2016**, *8*, 30294−30303.
(13) Zhu, X.; Zheng, H.; Wei, X.; Lin, Z.; Guo, L.; Qiu, B.; Chen, G. *Chem. Commun.* **2013**, *49*, 1276−1278.
(14) Zhou, H. C.; Long, J. R.; Yaghi, O. M. *Chem. Rev.* **2012**, *112*, 673−674.
(15) Xue, D.-X.; Wang, Q.; Bai, J. *Coord. Chem. Rev.* **2019**, *378*, 2−16.
(16) Fan, W.; Wang, X.; Xu, B.; Wang, Y.; Liu, D.; Zhang, M.; Shang, Y.; Dai, F.; Zhang, L.; Sun, D. *J. Mater. Chem. A* **2018**, *6*, 24486−24495.
(17) Liu, M.; Xie, K.; Nothling, M. D.; Gurr, P. A.; Tan, S. S. L.; Fu, Q.; Webley, P. A.; Qiao, G. G. *ACS Nano* **2018**, *12*, 11591−11599.
(18) Xu, X. Y.; Yan, B. *ACS Appl. Mater. Interfaces* **2015**, *7*, 721−729.
(19) Hao, J. N.; Yan, B. *Chem. Commun. (Cambridge, U. K.)* **2015**, *51*, 7737−7740.
(20) Jin, Y.; Tian, X.; Jin, L.; Cui, Y.; Liu, T.; Yu, Z.; Huo, X.; Cui, J.; Sun, C.; Wang, C.; Ning, J.; Zhang, B.; Feng, L.; Ma, X. *Anal. Chem.* **2018**, *90*, 3276−3283.
(21) Jiang, X. L.; Hou, S. L.; Jiao, Z. H.; Zhao, B. *Anal. Chem.* **2019**, *91*, 9754−9759.
(22) Chen, W. H.; Luo, G. F.; Vázquez-González, M.; Cazelles, R.; Sohn, Y. S.; Nechushtai, R.; Mandel, Y.; Willner, I. *ACS Nano* **2018**, *12*, 7538−7545.
(23) Gao, J.; Wang, C.; Tan, H. *J. Mater. Chem. B* **2017**, *5*, 7692−7700.
(24) Stubbs, A. W.; Braglia, L.; Borfecchia, E.; Meyer, R. J.; Román-Leshkov, Y.; Lamberti, C.; Dincă, M. *ACS Catal.* **2018**, *8*, 596−601.
(25) Riccò, R.; Liang, W.; Li, S.; Gassensmith, J. J.; Caruso, F.; Doonan, C.; Falcaro, P. *ACS Nano* **2018**, *12*, 13−23.
(26) Cao, C. S.; Shi, Y.; Xu, H.; Zhao, B. *Dalton Trans.* **2018**, *47*, 4545−4553.
(27) Yang, Z. R.; Wang, M. M.; Wang, X. S.; Yin, X. B. *Anal. Chem.* **2017**, *89*, 1930−1936.
(28) Di, M.; Shen, J.; Cui, Z.; Zhang, X.; Zhang, J. *New J. Chem.* **2019**, *43*, 4226−4234.
(29) Wang, Y. M.; Yang, Z. R.; Xiao, L.; Yin, X. B. *Anal. Chem.* **2018**, *90*, 5758−5763.
(30) Xu, X. Y.; Lian, X.; Hao, J. N.; Zhang, C.; Yan, B. *Adv. Mater.* **2017**, *29*, 1702298.
(31) Arici, M. *New J. Chem.* **2019**, *43*, 3690−3697.
(32) Zheng, H. Y.; Lian, X.; Qin, S. J.; Yan, B. *ACS Omega* **2018**, *3*, 12513−12519.
(33) Hou, S. L.; Dong, J.; Tang, M. H.; Jiang, X. L.; Jiao, Z. H.; Zhao, B. *Anal. Chem.* **2019**, *91*, 5455−5460.
(34) Yang, A. F.; Hou, S. L.; Shi, Y.; Yang, G. L.; Qin, D. B.; Zhao, B. *Inorg. Chem.* **2019**, *58*, 6356−6362.
(35) Wan, Y. T.; Zou, D. Z.; Cui, Y. J.; Yang, Y.; Qian, G. D. *J. Solid State Chem.* **2018**, *266*, 70−73.
(36) Li, L.; Chen, Q.; Niu, Z.; Zhou, X.; Yang, T.; Huang, W. *J. Mater. Chem. C* **2016**, *4*, 1900−1905.
(37) Ji, G.; Liu, J.; Gao, X.; Sun, W.; Wang, J.; Zhao, S.; Liu, Z. *J. Mater. Chem. A* **2017**, *5*, 10200−10205.
(38) Li, Y.; Ma, D.; Chen, C.; Chen, M.; Li, Z.; Wu, Y.; Zhu, S.; Peng, G. *J. Solid State Chem.* **2019**, *269*, 257−263.
(39) Chatterjee, A.; Banerjee, M.; Khandare, D. G.; Gawas, R. U.; Mascarenhas, S. C.; Ganguly, A.; Gupta, R.; Joshi, H. *Anal. Chem.* **2017**, *89*, 12698−12704.
(40) Matsushita, M.; Meijler, M. M.; Wirsching, P.; Lerner, R. A.; Janda, K. D. *Org. Lett.* **2005**, *7*, 4943−4946.
(41) Sarafraz Yazdi, A.; Banihashemi, S.; Es'haghi, Z. *Chromatographia* **2010**, *71*, 1049−1054.

https://dx.doi.org/10.1021/acs.analchem.9b05410
Anal. Chem. 2020, 92, 3366−3372